

THE TRANSFORMATION IN THE  $\gamma$ -PHASE OF THE Cu-Zn, Cu-Cd, Ag-Zn and Ag-Cd SYSTEMSP. Wallbrecht,<sup>(a)</sup> F. Balck,<sup>(b)</sup> R. Blachnik<sup>(c)</sup> and K.C. Mills<sup>(d)</sup><sup>(a)</sup> Anorg.Chem.Inst., T.U. Clausthal, W. Germany<sup>(b)</sup> Inst.Angew.Phys., T.U. Clausthal, W. Germany<sup>(c)</sup> Fachbereich 8 Chemie, G.H.Siegen, W. Germany<sup>(d)</sup> Division of Chemical Standards, National Physical Laboratory, Teddington, UK

(Received April 19, 1976)

1. Introduction

The  $\gamma$ -phase reported for the systems Cu-Zn, Cu-Cd, Ag-Zn and Ag-Cd occurs at a composition close to  $A_2B_3$  where A is Cu or Ag and B is Zn or Cd. Structures of the  $\gamma$  phase have been determined for the Cu-Zn and Cu-Cd systems (1) and for the Ag-Zn system (2). The phase boundary limits of the  $\gamma$ -phase for temperatures above 570 K have been reported for all four systems (3). However, the homogeneity ranges of the  $\gamma$ -phases are not known for temperatures below 370 K and are uncertain for the temperature interval (370 - 570 K). An anomaly in the electrical resistance-temperature curve for  $\gamma$ -brass has been observed (4,5) to occur in the range (520 - 550 K). Melikhov et al. (6) noted a discontinuity around 525 K in the lattice parameter-temperature plot for  $\gamma$ -brass, this was attributed to the transformation of a rhombic structure into a cubic structure. Küster (7) reported that a transformation occurred at about 590 K from measurements of the modulus of elasticity.

In this study the  $\gamma$ -phase transformation in the Cu-Zn, Cu-Cd, Ag-Zn and Ag-Cd system has been further investigated with measurements of electrical resistance and lattice constant (FB) and heat capacity (PW).

2. ExperimentalSample preparation

The single crystals were prepared from high purity metals (silver from Degussa/Hanau, copper/zinc/cadmium from Preussag AG, all 99.9995%). A detailed description of the method will be published shortly (8). The polycrystalline samples were prepared from weighed stoichiometric amounts of the same high purity metals. The two components were melted together in sealed, evacuated silica capsules and quenched into iced water. The samples were then homogenised 5 K below the solidus temperatures for 1 week and slowly cooled to room temperature. The products were crushed and pressed into discs. Any stored energy effects caused by the cold work were eliminated by further annealing.

Calorimetry

All differential scanning calorimetry (DSC) experiments were carried out with a Perkin-Elmer DSC-2. The specific heat mode was used in all cases (9). The DSC-output was stored on paper tape and the data were evaluated with the aid of a KDF-9 computer. A detailed description of the technique and the data evaluation has been reported previously (10)(11). Experiments with different heating rates (5, 20 and 40 K min<sup>-1</sup>) were carried out so that all registered temperatures could be extrapolated to temperatures corresponding to zero heating rate.

Resistance measurements

The electrical resistance was measured using an AC-method with lock-in-amplifier and a four-point probe.

X-ray and dilatation measurements

The lattice constants were measured by the rotating crystal method with  $CuK\alpha$ -radiation. Dilatation experiments were carried out with a silica-apparatus, a differential transformer was used as the pick-up.

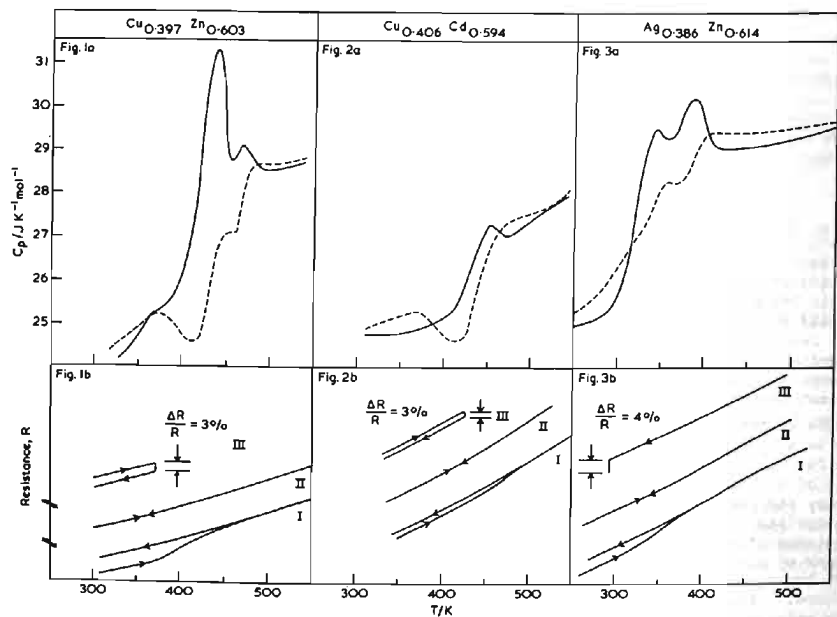


FIG. 1a,2a,3a. Heat capacity vs temperature, fully annealed samples, quenched samples.

FIG. 1b,2b,3b. Electrical resistance (arbitrary units) vs temperature.

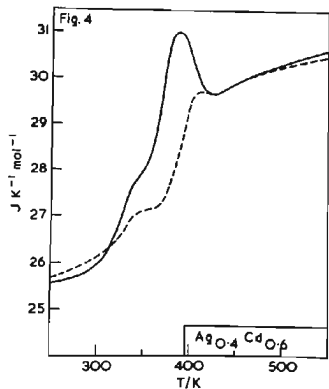


FIG. 4. Heat capacity vs temperature, — fully annealed sample, - - - quenched samples

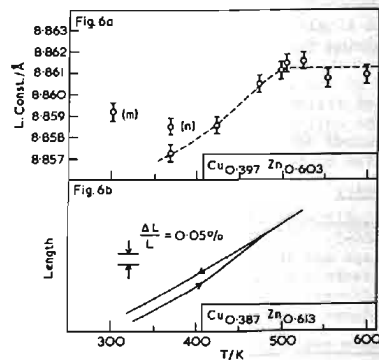


FIG.6 (a) Lattice constant vs temperature for  $\gamma$ -Cu Zn (b) Dilation vs temperature for  $\gamma$ -Cu Zn.

### 3. Results

One mole refers to the species  $A_xB_{1-x}$  where A is Cu or Ag and B is Zn or Cd. Temperatures are based on IPTS-68.

#### Heat capacity measurements

Heat capacity ( $C_p$ ) measurements shown in fig. 1a-3a were determined on single-crystals; the heat capacity values obtained with polycrystalline samples of identical composition showed no differences from those for single crystals. The heat capacity data for Ag<sub>0.4</sub>Cd<sub>0.6</sub> shown in fig. 4 were obtained on polycrystalline material only. The full lines in these figures refer to samples which had been fully annealed at temperatures below the transition temperature (7 days at 370 K for Cu Zn, 48 h at 380 K for Cu Cd, 48 h at 300 K for Ag Zn and 14 days at 300 K for Ag Cd). The dashed curves in these figures refer to samples quenched at 200 K min<sup>-1</sup> from 550 K to 300 K. The effect of composition upon the  $\gamma$  transformation in Cu Zn single crystals is clearly shown in fig. 5. The  $C_p(T)$  curves for all compositions possessed a  $C_p$  maximum and double peaks were observed for three compositions and for  $\gamma$ -Ag<sub>0.386</sub>Zn<sub>0.614</sub>. The highest temperature observed for the  $C_p$  peak occurred in an alloy of composition Cu<sub>0.377</sub>Zn<sub>0.623</sub>.

#### Electrical resistance measurements

The electrical resistance - temperature curves for single crystals of  $\gamma$ -Cu Zn,  $\gamma$ -Cu Cd and  $\gamma$ -Ag Zn are given in figs. 1b, 2b and 3b respectively. The  $R(T)$  curves shown in these figures refer to the following conditions:

Curve I: The electrical resistance of the annealed samples was measured at low heating rate (3 K min<sup>-1</sup>) and high cooling rate (30 K min<sup>-1</sup>). The resistance of the cooled ("quenched") samples were 3 - 4% above those of the annealed samples.

Curve II: The resistance of the "quenched" sample was then measured at high heating (10 K min<sup>-1</sup>) and cooling rates. The  $R(T)$  curve was identical for both heating and cooling runs indicating that the high electrical resistance of the "quenched" phase was maintained for the duration of the experiment.

Curve III: The samples were then annealed for 20 h at annealing temperatures (Cu Zn, 370 K; Cu Cd, 400 K; Ag Zn, 300 K) selected to lie below the transition temperature. This annealing produced a decrease in electrical resistance, associated with the transformation of the high-temperature,  $\gamma$  phase in the "quenched" sample into the equilibrium, low-temperature form. Thus the  $R(T)$  curve was unaffected by the fast cooling rate employed, as all measurements on the low-temperature,  $\gamma$ -phase were carried out below the transition temperature.

#### Lattice parameter measurements

A single crystal of  $\gamma$ -Cu Zn was subjected to one of the following annealing treatments, 48 h at 370 K, 15 h at 425 K and 475 K, 5 h at 500 K, 3 h at 525 K, 550 K and 590 K, and then quenched into water. Lattice constants,  $a$ , for the quenched samples were determined and are plotted against annealing temperature in fig. 6a. This  $a(T)$  relationship is fitted by a curve

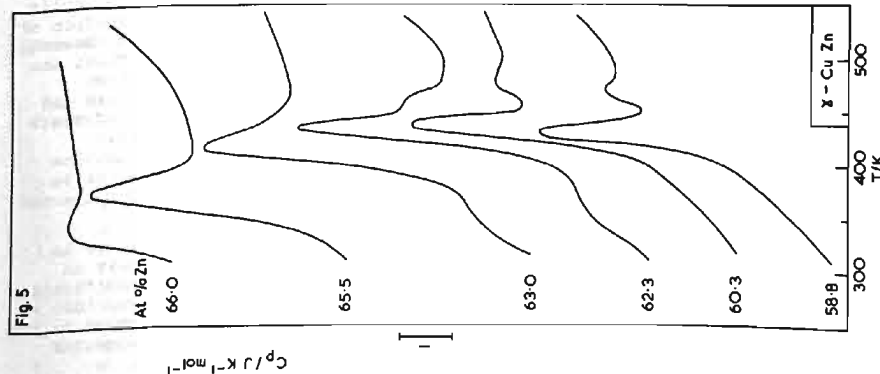


FIG. 5 Heat capacity vs temperature for various compositions within the  $\gamma$ -Cu Zn phase field.

to 500 K; for temperatures above 500 K the lattice parameter has a constant value. Incomplete annealing of the sample results in a high value for the lattice parameter as can be seen from the points (m) and (n) in fig 6a; these samples had been subjected to annealing periods of 60 days at 300 K and 24 h at 370 K, respectively. As all measurements were carried out at room temperature, the slope of the  $a(T)$  curve was unaffected by thermal expansion effects. The lattice parameter increased by 0.04% between 370 and 500 K. There were no significant changes in the diffraction patterns for 370 and 600 K. All back reflections were identified as those of  $\gamma$ -brass, hence there was no evidence for the presence of the low-temperature modification reported by Melikhov (6) in these samples.

#### Expansion coefficient measurements

The dilatation measurements for a single crystal of  $\gamma$ -Cu Zn, which had been annealed for 20 h at 370 K, are shown in fig. 6. The expansion coefficient increased between 400 K and 500 K and on rapid cooling the length of the quenched sample (high-temperature  $\gamma$  form) was larger than that for the annealed sample (low-temperature form) by about 0.05%, a value in line with that obtained from lattice constant measurements.

#### 4. Discussion

The results of the various measurements reported in this study all show quite clearly that a transition occurs at low temperatures in these alloys. The enthalpy of transition,  $\Delta H_t$ , and the temperature range where the transformation produces an anomaly in the  $C_p(T)$  curve are listed in Table 1. Neither the temperature ranges nor the enthalpies of the transitions in various alloys are strictly comparable as both quantities are dependent upon both composition (see fig.5)

TABLE 1  
Temperature Range and Enthalpy of the  $\gamma$ -phase Transformation

Alloy	$\text{Cu}_{0.603}\text{Zn}_{0.397}$	$\text{Ag}_{0.614}\text{Zn}_{0.386}$	$\text{Cu}_{0.594}\text{Cd}_{0.406}$	$\text{Ag}_{0.6}\text{Cd}_{0.4}$
Temperature Range/K	403 - 490 ( $\pm 5$ )	303 - 407 ( $\pm 5$ )	406 - 470 ( $\pm 5$ )	304 - 418 ( $\pm 5$ )
$\Delta H_t / \text{J K}^{-1} \text{mol}^{-1}$	$169 \pm 15$	$177 \pm 15$	$29 \pm 5$	$116 \pm 15$

and the annealing treatments. However, it can be seen from Table 1 that the  $\Delta H_t$  values are very small.

If the transition temperature is defined as the minimum temperature at which all the  $\gamma$ -phase transformations are complete then there is reasonable agreement between the temperatures recorded by various measurements for any specific alloy, eg for  $\gamma$ -Cu Zn, 490 K from fig. 1a, 500 K from fig. 6a, 475 K from fig. 6b and 480 K from curve I of fig. 1b. These temperatures are all lower than the other recorded transition temperatures 530 K (4) 550 K (5) 520 K (6) and 590 K (7). The discrepancy between the transition temperatures can be attributed to (i) the unsuitability of some methods, particularly dynamic techniques, for the determination of transition temperatures (ii) the effect of the thermal history of the sample, which was observed to have an effect on the shape of the  $C_p(T)$  curve in this study and could therefore affect the temperature dependency of other properties (iii) the criteria used for defining transition temperature, eg Imai (4) used the temperature at which the  $R(T)$  curve becomes linear again and Matsuda (5) the temperature at which the change takes place most rapidly. In the case of the data due to Melikhov et al. (6) there may also be compositional differences between their samples and those used here. If the lattice constants reported (6) are compared with lattice constant-composition data (12) it may be deduced that their sample had a composition close to the zinc-rich boundary of the  $\gamma$ -phase, where a transition temperature of 400 K would be expected from fig. 5.

The  $C_p(T)$  curves for quenched samples of  $\gamma$ -Cu Zn and  $\gamma$ -Cu Cd, denoted as dotted lines in fig. 1b and 2b, contain a  $C_p$  minimum at the onset of the transition range. This suggests an ordering process; one possible explanation is that the metastable, high-temperature modification is transformed ("ordered") to the low-temperature form, which subsequently re-transforms into the high temperature modification at higher temperatures. This behaviour was not observed in the silver alloys where the  $C_p(T)$  curves of the quenched samples resemble those of fully-annealed samples but correspond to a lower enthalpy of transition.

The nature of this transformation in the  $\gamma$ -phase is not known; several possible mechanisms exist (i) an order-disorder transformation (ii) a structural transformation (iii) a eutectoid transformation (iv) vacancy formation (v) short-range ordering effects. It would appear to be unlikely that the transformation is of the order-disorder type, as the experimental  $\Delta H_t$  values listed in Table 1 are more than an order of magnitude smaller than the values predicted for order-disorder transformations by the Bragg-Williams theory,  $\Delta H_t \approx 2 \text{ kJ mol}^{-1}$ . A rhombic modification of  $\gamma$ -Cu Zn has been reported (6) to occur below 520 K; no evidence of this modification was found in this study. Thus a structural transformation would appear improbable in  $\gamma$ -Cu Zn, as the X-ray data obtained in this study for the low-temperature form were identical with data reported for the high-temperature form of  $\gamma$ -Cu Zn. This fact would also appear to rule out the possibility of a eutectoid transformation. This is substantiated by the identification of the high temperature form of  $\gamma$ -Cu Zn as one of the products of the reported, low-temperature, eutectoid transformation for  $\beta$ -Cu Zn (13). The transformation is therefore probably associated with either a redistribution of vacancies or a short-range ordering effect.

A similar transformation to that reported here for the  $\gamma$ -phase has been observed in both  $\alpha$ -Cu Zn and  $\alpha$ -AgZn; Hirano et al. (14) reported a value for the enthalpy of transition,  $\Delta H_t = 270 + 20 \text{ J mol}^{-1}$  for  $\alpha$ -Cu Zn which is of the same order of magnitude as the  $\Delta H_t$  values listed in Table 1. They suggested that G-P zones were formed in  $\alpha$ -Cu Zn and the enthalpy of transformation was associated with their destruction. Clarebrough et al. (15-19) reported results obtained by differential calorimetry, electrical resistance, density and lattice parameter studies for slowly-cooled, quenched and annealed samples of  $\alpha$ -Cu Zn and  $\alpha$ -Ag Zn. The results reported in this study of  $\alpha$ -phases (15-19) are very similar to those recorded here for the  $\gamma$ -phases. Clarebrough et al. concluded that the transformation was a short range order effect caused by the dynamic nature of the experiments, which do not allow the true equilibrium degree of order for any specific temperature below the transition temperature to be developed in the sample. They also concluded on the basis of density measurements that the transformation could not be due to the redistribution of vacancies alone but they were able to show that the annealing process was aided considerably by vacancies in the lattice.

The great similarity in the results of the studies on the  $\alpha$ -phase and the  $\gamma$ -phase suggest that the  $\gamma$ -phase transformation is also caused by the destruction of short range order in the sample. Thus  $\gamma$ -phase samples which had been subjected to long-annealing treatments would produce a greater degree of order in the sample and hence would require a larger enthalpy ( $\Delta H_t$ ) to disorder. The atomic mobility of the elements is obviously a key factor in this behaviour of the  $\gamma$ -phase; a relatively high value has been reported for the chemical diffusion coefficient in  $\gamma$ -Cu Zn (20,21). However, it is known that the chemical diffusion coefficient in Cu Zn alloys increases with increasing zinc content. Hence the temperature of the onset and completion of the  $\gamma$ -phase transformation would be expected to decrease with increasing zinc content; this effect is clearly shown in fig. 5. Moreover, the chemical diffusion coefficient in Ag Zn is known to be greater than that in Cu Zn alloys. The high atomic mobility in  $\gamma$ -Ag Zn and  $\gamma$ -Ag Cd accounts for the fact that the ordering process occurs readily for annealing temperatures as low as 300 K. It also accounts for the absence of minima in the  $C_p(T)$  curves for quenched samples of  $\gamma$ -Ag Zn and  $\gamma$ -Ag Cd where the ordering process is considerably more rapid than that in  $\gamma$ -Cu Zn and  $\gamma$ -Cu Cd alloys.

Thus we conclude that these  $\gamma$ -phase transformations are most probably a short range ordering phenomenon. Further work is now in progress to confirm this unequivocally.

#### Acknowledgement

We thank J. Simon for the single crystals, Dr M J Richardson, Dr G Frommeyer for fruitful discussions and Deutsche Forschungs Gemeinschaft and Fond der Chemie for financial support.

#### References

- J.K. Brandon, R.Y. Brizard, P.C. Chien, R.K. McMillan and W.B. Pearson, Acta cryst. B30, 1412 (1974).
- R.E. Marsh, Acta cryst. 7, 379 (1954).
- M. Hansen and K. Anderko, Constitution of Binary Alloys, McGraw-Hill, Princeton, N.J. (1958).
- H. Imai, Sci. Rep. Tohoku Univ., 11, 313 (1922).
- T. Matsuda, Sci. Rep. Tohoku Univ., 11, 223 (1922).
- V.D. Melikhov, K. Kasymbekova, T.P. Polyakova and A.A. Presnyakov, Fizika Metall., 16, No. 5, 700 (1922).
- W. Köster, Z. Metallk., 32, 155 (1940).

8. J. Simon to be published.
9. B. Wunderlich, *J. Phys. Chem.* 69,2078 (1965).
10. K.C. Mills and M.J. Richardson, *Thermochimica Acta*, 6, 427 (1973).
11. M.J. Richardson and P. Burrington, *J. Thermal Analysis*, 6, 345 (1974).
12. A. Johanson and A. Westgren, *Z. Metallwirtsch.* 12, 385 (1933).
13. G. Shinoda and Y. Amano, *Trans. Jap. Inst. Metals*, 1,54 (1960).
14. K. Hirano, H. Maniwa and Y. Takagi, *J. Phys.Soc. Japan*, 10, 909 (1955).
15. L.M. Clarebrough, M.E. Hargreaves and M.H. Loretto, *Proc. Roy. Soc.*, A.257,326 (1960).
16. L.M. Clarebrough, M.E. Hargreaves and M.H. Loretto, *Proc. Roy. Soc.*, A.257,338 (1960).
17. L.M. Clarebrough, M.E. Hargreaves and M.H. Loretto, *Proc. Roy. Soc.*, A.257,363 (1960).
18. L.M. Clarebrough, M.E. Hargreaves and M.H. Loretto, *Proc. Roy. Soc.*, A.261,500 (1960).
19. L.M. Clarebrough, M.E. Hargreaves and M.H. Loretto, *J. Austral. Inst. Metals*, 8,308 (1963).
20. R.F. Mehl and C.F. Lutz, *Trans. Am. Inst. Min. Metall. Engrs.* 221,561 (1961).
21. G. Schwitzgebel, *Acta metall.* 20, 1297 (1972).